

ORIGINAL PAPER

Molecular Phylogeny of the Benthic Dinoflagellate Genus *Amphidiniopsis* and its Relationships with the Family Protopteridiniaceae



Aika Yamaguchi^{a,1}, Sadaaki Yoshimatsu^b, Mona Hoppenrath^c,
Kevin C. Wakeman^d, and Hiroshi Kawai^a

^aKobe University Research Center for Inland Seas, Kobe 657-8501, Japan

^b2298-28 Yashima Nishimachi, Takamatsu, Kagawa 761-0113, Japan

^cSenckenberg am Meer, German Centre for Marine Biodiversity Research, Südstrand 44,
D-26382 Wilhelmshaven, Germany

^dDepartment of Biological Sciences, Faculty of Science, Hokkaido University, North 10,
West 8, Sapporo 060-0810, Japan

Submitted May 10, 2016; received in revised form August 30, 2016; Accepted September 24, 2016
Monitoring Editor: Laure Guillou

The genus *Amphidiniopsis* is a benthic (sand-dwelling) lineage of thecate dinoflagellates, containing 19 morphologically diverse species. Past work has shown that some *Amphidiniopsis* species form a clade with the sand-dwelling *Herdmania litoralis* as well as some planktonic species in the family Protopteridiniaceae (i.e. the *Monovela* group). Still, our contemporary knowledge regarding *Amphidiniopsis* is limited, compared to the Protopteridiniaceae. To this end, we obtained 18S rDNA data from seven *Amphidiniopsis* species and a part of the 28S rDNA from four *Amphidiniopsis* species, with the goal of improving our understanding of phylogenetic relationships among *Amphidiniopsis* and the *Monovela* group. Results from the molecular phylogenetic analyses showed that *Amphidiniopsis* spp., with the exception of *A. cf. arenaria*, *H. litoralis*, and members within the *Monovela* group formed a single clade. Within the clade, relationships among *Amphidiniopsis* spp. and the *Monovela* group were more complicated — some subclades contained both representatives of *Amphidiniopsis* and the *Monovela* group. Our study suggests that habitat (benthic or planktonic), as well as traditionally used, general morphological characteristics, do not reflect molecular phylogenetic relationships, and that the taxonomy of the sand-dwelling genus *Amphidiniopsis*, and the planktonic family Protopteridiniaceae, should be reconsidered simultaneously.

© 2016 Elsevier GmbH. All rights reserved.

Key words: *Amphidiniopsis*; *Archaeoperidinium*; *Herdmania*; heterotrophic dinoflagellate; molecular phylogeny; Protopteridiniaceae.

Introduction

The genus *Amphidiniopsis* was established by Wołoszyńska (1928) and currently contains 19

¹Correspondence author; fax +81 78 803 6698
e-mail aika@harbor.kobe-u.ac.jp (A. Yamaguchi).

species (Hoppenrath et al. 2014). This genus is heterotrophic and has a smaller epitheca, compared to its hypotheca. Although the type species, *Amphidiniopsis kofoidii* Wołoszyńska, was found in a littoral plankton sample from the Baltic Sea (Wołoszyńska 1928), most of the *Amphidiniopsis* species have been described from sandy sediments, and there are records that *A. kofoidii* has also been observed from marine sand (Hoppenrath et al. 2014). Therefore, this genus is recognized as being benthic/sand-dwelling.

Morphologically, *Amphidiniopsis* contains diverse range of species. Hoppenrath et al. (2012, 2014) proposed three major groups in the genus *Amphidiniopsis* (i.e. Group 1, 2 and 3). These three groups were distinguished by cell flattening (lateral or dorsoventral), cingulum morphology (complete or “incomplete”), the apical hook (present or absent), the number of anterior intercalary plates, the relative position of the second intercalary plate and sulcal morphology (Hoppenrath et al. 2012, 2014).

Gómez et al. (2011) obtained 18S rDNA data from *Amphidiniopsis hirsuta* (Balech) Dodge and *A. swedmarkii* (Balech) Dodge in order to analyze the systematic position of the genus *Amphidiniopsis* and its phylogenetic affinity to other dinoflagellates. At a similar time, Hoppenrath et al. (2012) described a new *Amphidiniopsis* species, *Amphidiniopsis rotundata* Hoppenrath et Selina, and also analyzed the 18S rDNA from this novel isolate. The resulting 18S rDNA phylogeny showed that the sand-dwelling *Amphidiniopsis*, *Thecadinium dragescoi* Balech, and *Herdmania littoralis* Dodge (Hoppenrath 2000a), together with the planktonic *Archaeoperidinium minutum* (Kofoid) Jørgensen, formed a strongly supported clade. Within this clade, *A. hirsuta* and *A. swedmarkii* grouped together as sister species (Gómez et al. 2011), and *T. dragescoi* and *A. rotundata* formed a sister group (Hoppenrath et al. 2012). According to these phylogenetic results, and with support from morphological characters, Hoppenrath et al. (2012) recombined *Thecadinium dragescoi* as *Amphidiniopsis dragescoi* (Balech) Hoppenrath, Selina, A. Yamaguchi et Leander.

The planktonic *Archaeoperidinium minutum* was initially classified as *Protoperidinium minutum* (Kofoid) Loeblich III, because its thecate cell has a plate pattern diagnostic for the heterotrophic and planktonic genus *Protoperidinium*. Mertens et al. (2012) and Liu et al. (2015) described new species of *Archaeoperidinium* through incubation experiments of the cysts collected from coastal sediment samples. The cysts of *Archaeoperidinium* have

a round shape, brown color and many spines (Liu et al. 2015; Mertens et al. 2012; Ribeiro et al. 2010). Similar cysts have been found in relative abundance in oceanic sediments, and they are called “spiny round brown cysts” (Mertens et al., 2012). Through the cyst incubation studies of spiny round brown cysts, considerable amounts of morphological and molecular phylogenetic data have been generated and analyzed revealing new species (e.g. Kawami et al. 2009; Liu et al. 2013; Mertens et al. 2013, 2015a; Potvin et al. 2013). Germinated motile cells from these cysts have morphological features related to the *Monovela* group proposed by Abé (1936, 1981). Molecular phylogenetic analyses including representatives of the *Monovela* group showed that they formed a clade with *H. littoralis*, *A. dragescoi* and *Archaeoperidinium* spp., and had phylogenetic position separate from *Protoperidinium sensu stricto* (Liu et al. 2013; Mertens et al. 2013, 2015a; Potvin et al. 2013). Within the *Monovela* group, molecular phylogenetics have identified three subgroups (clades) (*Americanum*, *Minutum* and *Monovelum*) (e.g. Liu et al. 2013; Matsuoka and Kawami 2013; Mertens et al. 2015b).

Besides a number of planktonic species within the family Protoperidiniaceae (the *Monovela* group), phylogenetic analyses examining sand-dwelling species related to *H. littoralis* and *Amphidiniopsis* have not been performed after Gómez et al. (2011) and Hoppenrath et al. (2012). To this end, we obtained 18S rDNA sequencing data from seven species of *Amphidiniopsis* (six of these being from species never before sequenced) and also part of 28S rDNA data from four *Amphidiniopsis* species, with the aim of better understanding the phylogenetic relationships among the sand-dwelling genus *Amphidiniopsis* and the members of the planktonic family Protoperidiniaceae. We performed phylogenetic analyses with the recently published data of the family Protoperidiniaceae.

Results

Morphology of *Amphidiniopsis* spp. Used for Single-cell Polymerase Chain Reaction (SC-PCR)

Cells of *Amphidiniopsis* cf. *arenaria* isolated for SC-PCR (*A. cf. arenaria*, isolate number 1, 2, see Table 1) were oval with flattened anterior end and the tapered posterior end (Fig. 1 A, B, E). The cells were laterally flattened (Fig. 1A, C-E). A button-like apical notch was observed on the epitheca (Fig. 1A, E). The cingulum ascended, and the sul-

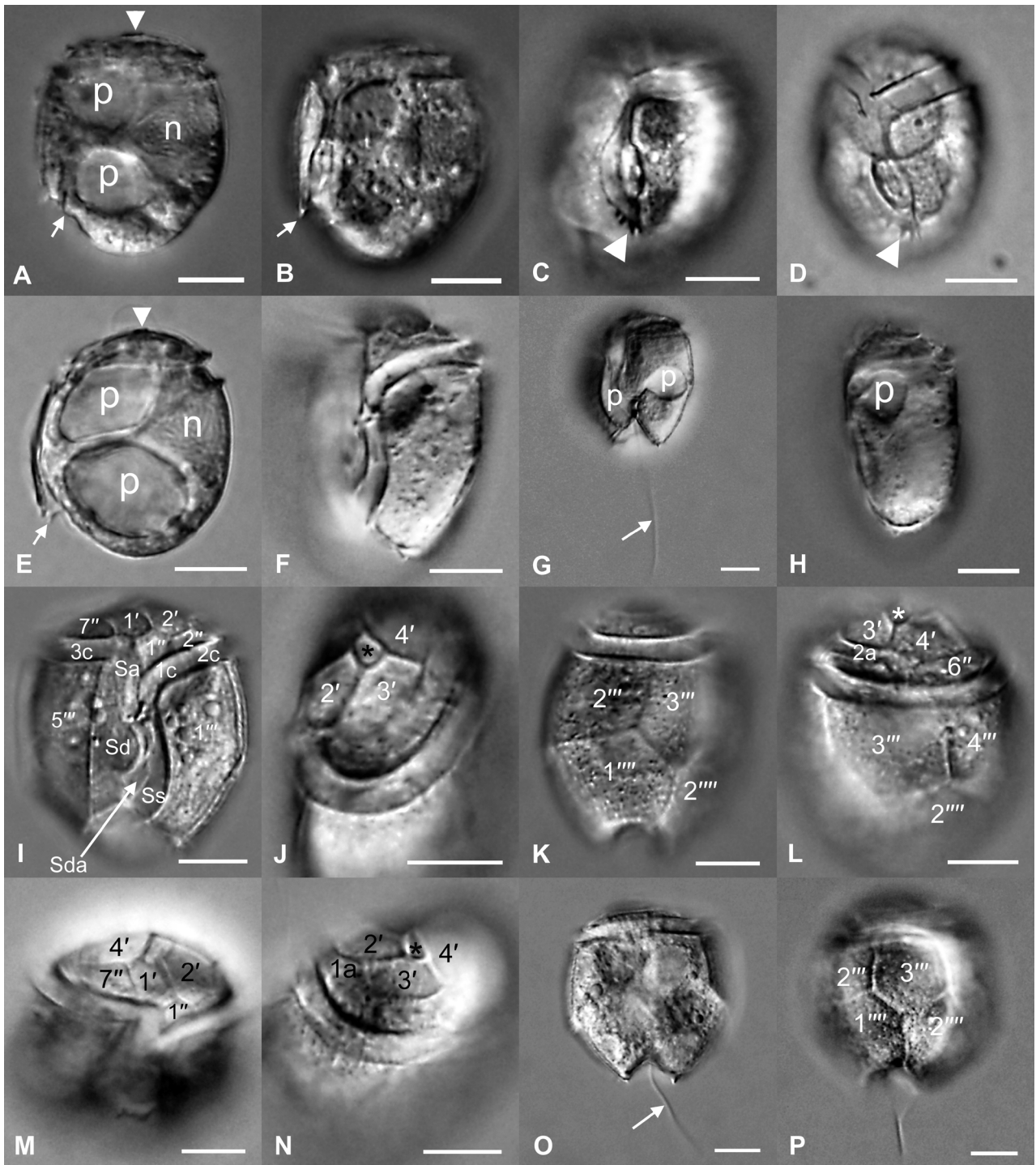


Figure 1. Light micrographs of the single-cells of *Amphidiniopsis* spp. used for rDNA sequencing (scale bars = 10 μ m). **A-E)** *Amphidiniopsis* cf. *arenaria*. **A)** Left view of *A.* cf. *arenaria* 1 showing the button-like apical notch (arrowhead), the ventral spine (arrow), the nucleus (n) and two pusules (p). **B)** Left view of *A.* cf. *arenaria* 1 showing the cingulum, the sulcus and the ventral spine (arrow). **C)** Ventral view of *A.* cf. *arenaria* 1 showing the wing-like structure (arrowhead). **D)** Ventral view of *A.* cf. *arenaria* 2 showing the wing-like structure (arrowhead). **E)** Left view of *A.* cf. *arenaria* 2 showing the button-like apical notch (arrowhead), the ventral spine (arrow), the nucleus (n) and two pusules (p). **F-P)** *Amphidiniopsis hexagona*. **F)** Left ventral view of *A.* *hexagona*

Table 1. Sampling data and accession numbers of *Amphidiniopsis* species.

Taxon	Isolate number	Collection date	Site	Accession number (18S)	Accession number (28S)
<i>Amphidiniopsis</i> cf. <i>arenaria</i>	1	18-Apr-14	Kannoura	LC191221	LC191240
	2	18-Apr-14	Kannoura	LC191222	LC191241
<i>Amphidiniopsis hexagona</i>	7	21-Aug-14	Oohama	LC191223	
	8	21-Aug-14	Oohama	LC191224	
	9	21-Aug-14	Oohama	LC191225	
<i>Amphidiniopsis</i> cf. <i>kofoidii</i>	BB3	16-Apr-07	Boundary Bay	LC191226	
<i>Amphidiniopsis korewalensis</i>	1	5-Oct-14	Tamamo-jyo	LC191227	LC191242
	4	5-Oct-14	Tamamo-jyo	LC191228	LC191243
	6	5-Oct-14	Tamamo-jyo	LC191229	LC191244
	7	5-Oct-14	Tamamo-jyo	LC191230	LC191245
	8	5-Oct-14	Tamamo-jyo	LC191231	LC191246
<i>Amphidiniopsis rotundata</i>	1	18-Apr-14	Kannoura	LC191232	LC191247
<i>Amphidiniopsis uroensis</i>	4	30-Apr-14	Suma-no-ura	LC191233	LC191248
	6	30-Apr-14	Maiko	LC191234	LC191249
	8	30-Apr-14	Maiko	LC191235	LC191250
	11	30-Apr-14	Maiko	LC191236	LC191251
	BB8	16-Apr-07	Boundary Bay	LC191237	
<i>Amphidiniopsis</i> spec.	1	16-Jun-07	Sandcut Beach	LC191238	
	6	16-Jun-07	Sandcut Beach	LC191239	

cus extended from the cingulum to the antapex, tilting to the left (Fig. 1D). There were two large pusules at the ventral side of the cell (Fig. 1A, E). The nucleus was positioned in the dorsal side, at the anterior end of the hypotheca (Fig. 1A, E). The ventral spine in the lower part of the hypotheca was observed in the lateral view of the cell (Fig. 1A, B, E). A wing-like structure was observed in the lower part of hypotheca which surrounded the posterior part of the sulcus (Fig. 1C, D).

Cells of *Amphidiniopsis hexagona* (*A. hexagona*, isolate number 7-9, see Table 1) that were isolated for SC-PCR were dorsoventrally flattened

and hexagonal in ventral view (Fig. 1G, H). The apical pore plate was surrounded by four apical plates (1'-4') (Fig. 1J, L, N). The second intercalary plate was long and narrow (Fig. 1L). The cingulum ascended, displaced by its own width (Fig. 1I, M). The sulcus was curved to the left side of the cell (Fig. 1F, I). The hypotheca consisted of five postcingular (1'''-5''') and two antapical plates (1''', 2''') (Fig. 1I, K, L, P). The antapex was deeply notched (Fig. 1G, I, O, P). The first and the fifth postcingular plate (1''', 5''') were large and occupied most of the ventral side of the cell (Fig. 1I). The third postcingular plate (3''') was five-sided, symmetrical

7 showing the curved sulcus. **G**) *A. hexagona* 7 showing the pusule (p) and the flagellum (arrow). **H**) Left view of *A. hexagona* 7 showing the pusule (p). **I**) Ventral view of *A. hexagona* 8 showing the anterior plates (1', 2'), the precingular plates (1'', 2'', 7''), cingular plates (1c-3c), the anterior sulcal plate (Sa), the right sulcal plate (Sd), the right accessory sulcal plate (Sda), the left sulcal plate (Ss) and the post cingular plates (1''', 5'''). **J**) Left apical view of *A. hexagona* 8 showing the plates and the apical pore plate (*). **K**) Left dorsal view of the hypotheca of *A. hexagona* 8 showing the postcingular plates (2''', 3''') and the antapical plates (1''', 2'''). **L**) Right dorsal view of *A. hexagona* 8 showing the apical pore plate (*), the apical plates (3', 4'), the second anterior intercalary plate (2a), the sixth precingular plate (6''), postcingular plates (3''', 4''') and the second antapical plate (2'''). **M**) Oblique ventro-apical view of *A. hexagona* 9 showing the apical plates (1', 2', 4') and the precingular plates (1'', 7''). **N**) Dorso-apical view of *A. hexagona* 9 showing the apical pore plate (*), the apical plates (2'-4') and the first anterior intercalary plate (1a). **O**) Dorsal hypotheca view of *A. hexagona* 9 showing the flagellum (arrow). **P**) Dorsal hypotheca view of *A. hexagona* 9 showing the postcingular plates (2''', 3''') and antapical plates (1''', 2''').

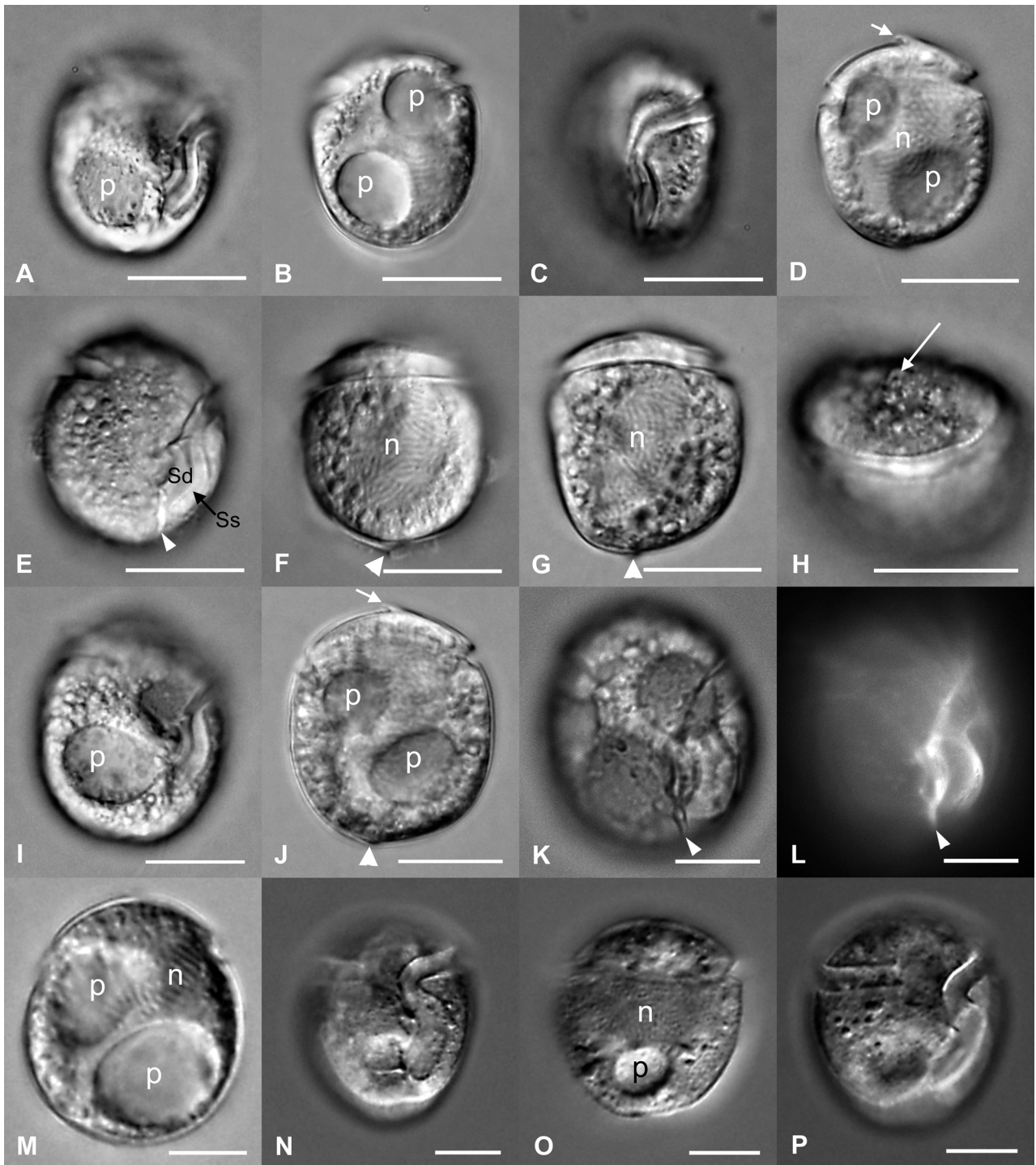


Figure 2. Light micrographs of the single-cells of *Amphidiniopsis* spp. used for rDNA sequencing (scale bars = 10 μ m). **A-M)** *Amphidiniopsis korewalensis*. **A)** Ventral view of *A. korewalensis* 1 showing the sulcus and the pusule (p). **B)** Whole cell view of *A. korewalensis* 1 showing two pusules (p). **C)** Left ventral view of *A. korewalensis* 1 showing the sulcus. **D)** Dorsal view of *A. korewalensis* 1 showing two pusules (p), the nucleus (n) and the apical notch (arrow). **E)** Ventral view of *A. korewalensis* 4 showing the incomplete cingulum, right and left sulcal plates (Sd, Ss) and the sulcal hook (arrowhead). **F)** Dorsal hypotheca of *A. korewalensis* 4 showing the nucleus (n) and the small bump at the posterior end (arrowhead). **G)** Dorsal hypotheca of *A. korewalensis*

and pointed posteriorly, and was positioned central to the posterior dorsal part (Fig. 1K, L, P). The first and the second antapical plates (1^{'''}, 2^{'''}) were equal in size and arranged symmetrically (Fig. 1P).

Cells of *Amphidiniopsis korewalensis* (*A. korewalensis*, isolate number 1, 4, 6-8, see Table 1) isolated for SC-PCR were ovoid in the ventral and dorsal views, with an apical notch pointing to the left side (Fig. 2B, D, E, J, K, M). Cells were flattened dorsoventrally (Fig. 2C, H). The large nucleus was positioned centrally within the cell (Fig. 2D, F, G). Two pusules were observed; one was positioned upper-left; another lower-right (Fig. 2B, D, I, J, M). Thecal plates were thin and their sutures were difficult to observe by light microscopy. No conspicuous ornamentation was observed on the thecal plates. The cingulum was incomplete (Fig. 2E, K), and the sulcus was broad and curved in an S-shape (Fig. 2A, C, E, I, K, L). The sulcal hook was positioned at the posterior right side of the sulcus (Fig. 2E, K, L). There was a small bump at the posterior end, which made the cell-shape of the posterior end pointed (Fig. 2F, G, J).

The cell of *Amphidiniopsis rotundata* (*A. rotundata*, isolate number 1, see Table 1) isolated for SC-PCR was ovoid and the nucleus positioned in the middle of the cell (Fig. 2O). The cell did not have an apical hook, nor posterior protrusions (Fig. 2N-P). The sulcus was wide and curved in an S-shape (Fig. 2N, P). The cingulum ascended about half the cingular width (Fig. 2P). One pusule was positioned at the posterior part (Fig. 2O).

Cells of *Amphidiniopsis uroensis* (*A. uroensis*, isolate number 4, 6, 8, 11, see Table 1) that were isolated for SC-PCR were dorsoventrally flattened (Fig. 3H), with an apical notch pointing to the left lateral cell side (Fig. 3B, C, G). Images acquired by epifluorescence microscopy showed that thecal surfaces were covered with small dots (Fig. 3C-F). The cingulum was incomplete as the anterior sulcal plate (Sa) and the right sulcal plate (Sd) attached to the first cingular plate (1c) and the third cingular plate (3c), respectively (Fig. 3D, E). The Sd looked like the shape of a "3" in fluorescent images (Fig. 3C). The sixth precingular plate (6^{''}) was nar-

row and long in the lateral direction, and attached to the Sa (Fig. 3D). The first and fifth postcingular plates (1^{'''}, 5^{'''}) were large and occupy most of the ventral side of the hypotheca (Fig. 3D, E). The third postcingular plate (3^{'''}) was pentagonal and positioned at the central part of the dorsal hypotheca (Fig. 3F).

Cells isolated in Canada were separated (some for the DNA extraction and others for SEM observations). They showed a typical-described morphology for the species (Fig. 4A-D) with a smooth apical hook.

Amphidiniopsis cf. *kofoidii* (Fig. 4E, F) from Canada was laterally flattened, with smooth thecal plates, containing pores (two size classes). No apical hook or antapical spines were observed, but a ventral spine was found. Intercalary bands were transversely striated in old specimens. The plate formula was: APC 4' 3a 8/9''? c? s? 5''' 2'''. *Amphidiniopsis* spec. (Fig. 4G, H) from Canada was a large (about 58 µm long), elongated, and dorsoventrally flattened species, having an apical hook and a cingulum that looked incomplete in the light microscope. No ornamentation or further cell appendages like spines were visible. The sulcus looked characteristically curved and shifted to the left side of the cell. The large nucleus was located in the central hyposome.

Phylogenetic Analysis of 18S rDNA

Nine *Amphidiniopsis* species (*A. dragescoi*, *A. hexagona*, *A. hirsuta*, *Amphidiniopsis* cf. *kofoidii*, *A. korewalensis*, *A. rotundata*, *A. swedmarkii*, *A. uroensis*, and *A. spec.*) were contained in a single clade, with two species of *Archaeoperidinium*, *Herdmania litoralis*, *Protoperidinium monovelum*, and the five species of the *Americanum* subgroup with the highest statistical support (Clade X, Fig. 5). One species of *Amphidiniopsis*, *A. cf. arenaria*, was not included in this clade and did not show any close relationship with the other dinoflagellates (Fig. 5). In Clade X, *Protoperidinium monovelum* and *A. rotundata* formed a clade with 99% ML bootstrap and 1.00 Bayesian PP.

6 showing the nucleus (n) and the small bump at the posterior end (arrowhead). **H**) Dorso-apical view of *A. korewalensis* 6 showing the apical pore plate (arrow). **I**) Ventral view of *A. korewalensis* 7 showing the sulcus and the pusule (p). **J**) Whole cell view of *A. korewalensis* 7 showing the apical notch (arrow), two pusules (p) and the small bump at the posterior end (arrowhead). **K**) Ventral view of *A. korewalensis* 8 showing the sulcal hook (arrowhead). **L**) The fluorescent micrograph of the ventral view of *A. korewalensis* 8 showing the sulcal hook (arrowhead). **M**) Dorsal view of *A. korewalensis* 8 showing two pusules (p) and the nucleus (n). **N-P**) *Amphidiniopsis rotundata* 1. **N**) Ventral view showing the sulcus. **O**) Whole cell view showing the nucleus (n) and the pusule (p). **P**) Ventral view showing the incomplete cingulum.

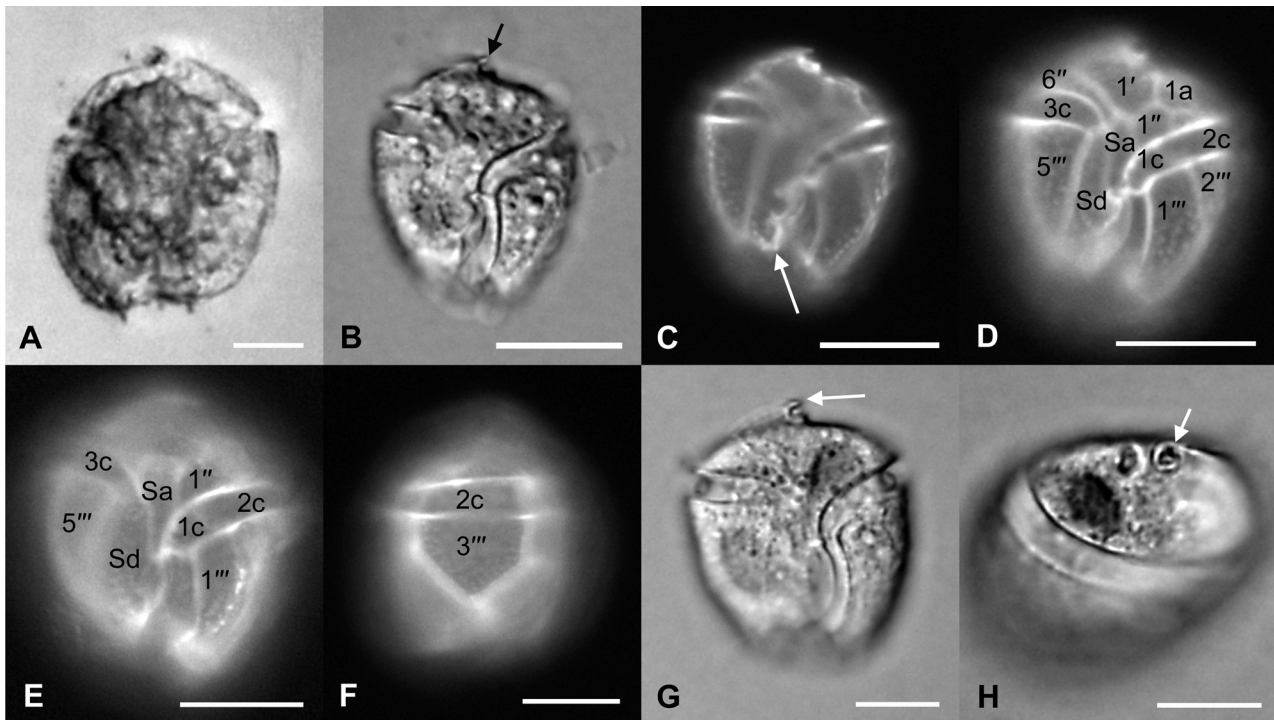


Figure 3. Light micrographs of the single-cells of *Amphidiniopsis uroensis* used for rDNA sequencing (scale bars = 10 μ m). **A)** Whole cell view of *A. uroensis* 4. **B)** Ventral view of *A. uroensis* 6 showing the apical notch (arrow). **C)** Epifluorescence micrograph of the ventral view of *A. uroensis* 6 showing the shape of “3” in the left edge of the right sulcal plate (arrow). **D)** Epifluorescence micrograph of *A. uroensis* 6 showing the first apical plate (1'), the first anterior intercalary plate (1a), precingular plates (1'', 6''), the anterior sulcal plate (Sa), the right sulcal plate (Sd), the cinglar plates (1c-3c) and the postcingular plates (1''', 2''', 5'''). **E)** Epifluorescence micrograph of *A. uroensis* 8 showing the 1'', the Sa, the Sd, the cinglar plates (1c-3c), and the postcingular plates (1''', 5'''). **F)** Epifluorescence micrograph of *A. uroensis* 8 showing the second cingular plate (2) and the third postcingular plate (3'''). **G)** The ventral view of *A. uroensis* 11 showing the apical notch (arrow). **H)** The dorso-apical view of *A. uroensis* 11 showing the apical notch (arrow).

Amphidiniopsis swedmarkii, *A. hirsuta* and *A. hexagona* formed a clade with 85% ML bootstrap support and 1.00 Bayesian PP. *Amphidiniopsis uroensis*, *A. korewalensis*, *Amphidiniopsis* spec., *A. cf. kofoidii*, and the *Americanum* subgroup formed a clade with 76% ML bootstrap and 1.00 Bayesian PP. The nodes of the branches throughout Clade X were not well supported. Outside of Clade X, eight species of *Protoperidinium sensu stricto* formed a clade with robust statistical support. The two species within the section *Oceanica* (*Protoperidinium claudicans* and *P. depressum*) formed a clade with 95% ML bootstrap and 1.00 Bayesian PP. Members of the diplopsalids were not monophyletic. The two clades comprised of the genera *Niea* and *Qia*, and *Diplopsalopsis bomba* and *Gotoius excentricus* had high statistical support; These two clades grouped together as sister lineages, with 84% ML bootstrap support and 1.00 Bayesian PP.

Phylogenetic Analysis of 28S rDNA

Three *Amphidiniopsis* species (*A. korewalensis*, *A. rotundata* and *A. uroensis*) were included in the clade, along with two species of *Archaeperidinium*, *Herdmania litoralis*, *Protoperidinium monovelum*, and the six species of the *Americanum* subgroup with 95% ML bootstrap support and 1.00 Bayesian PP.

Amphidiniopsis cf. *arenaria* was not included in Clade Y and did not group with high support with other dinoflagellates (Fig. 6). In Clade Y, *Protoperidinium monovelum*, *P. lewisiae* and *A. rotundata* formed a clade with 98% ML bootstrap and 1.00 Bayesian PP. *Amphidiniopsis uroensis*, *A. korewalensis* and the *Americanum* subgroup formed a clade with 94% ML bootstrap support and 1.0 Bayesian PP. In this clade, *A. uroensis* and *A. korewalensis* formed a clade with 98% ML bootstrap support and 1.00 Bayesian PP. Outside of Clade

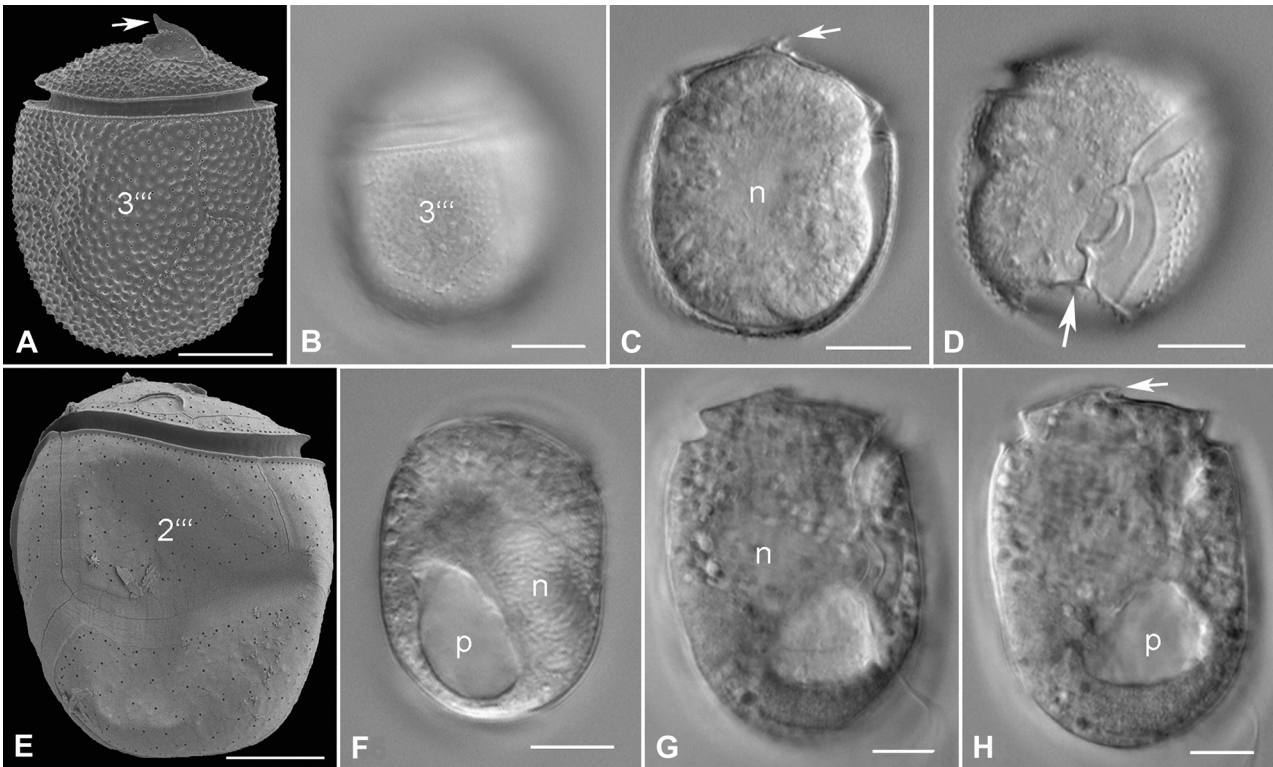


Figure 4. *Amphidiniopsis* species from Canada (scale bars = 10 μm). **A-D)** *A. uroensis*. **A)** Scanning electron micrograph of a cell in dorsal view. Note the apical notch (arrow). **B-D)** Light micrographs. **B)** Dorsal view showing the characteristic 3''' plate. **C)** Whole cell view showing the nucleus (n) in the cell centre and the apical notch (arrow). **D)** Ventral view, note the "3"-shape of the right sulcal area (large arrow). **E-F)** *A. cf. kofoidii*. **E)** Scanning electron micrograph of a cell in left lateral view. **F)** Light micrograph of a cell in left lateral view. Note the pusule (p) and nucleus (n). **G-H)** *A. spec.* **G)** Ventral view showing the sulcus shifted to the left and the nucleus (n) in a right mid cell position. **H)** Whole cell view showing one large pusule (p) and a smaller above; note the apical notch (arrow).

Y, nine species of *Protoperidinium sensu stricto* formed a clade with 91% ML bootstrap support and 1.0 Bayesian PP. Members of the diplopsalids were not monophyletic. The genera *Niea* and *Qia* were closely related. In addition with this *Niea* and *Qia* clade, *Diplopsalopsis ovata*, *D. bomba* and *Gotoius excentricus* formed a clade with 97% ML bootstrap support and 1.00 Bayesian PP.

Discussion

The phylogenetic analyses of 18S rDNA in the present study included ten species of *Amphidiniopsis*. This study also analyzed 28S rDNA from four *Amphidiniopsis* species for the first time. Both 18S and 28S rDNA results showed that those *Amphidiniopsis* spp. did not form a single clade and suggested a more complicated relationship between these species and the planktonic family

Protoperidiniaceae (Figs 5, 6). In the present 18S rDNA phylogeny, nine *Amphidiniopsis* species (*A. dragescoi*, *A. hexagona*, *A. hirsuta*, *A. cf. kofoidii*, *A. korewalensis*, *A. rotundata*, *A. swedmarkii*, *A. uroensis* and *Amphidiniopsis spec.*) were included in Clade X, which contains both the benthic species (these nine *Amphidiniopsis* species and *Herdmania litoralis*) and the members of the planktonic *Monovela* group of the family Protoperidiniaceae (Fig. 5). The 28S rDNA phylogeny also showed similar results. Three *Amphidiniopsis* species (*A. korewalensis*, *A. rotundata* and *A. uroensis*) in the 28S rDNA analysis were included in Clade Y, which contains both the sand-dwelling species (these three *Amphidiniopsis* species and *H. litoralis*) and the members of the *Monovela* group (Fig. 6). In both the 18S and 28S rDNA phylogenetic results, *A. cf. arenaria* was not included in Clade X nor Y; its phylogenetic position was unresolved (Figs 5, 6).

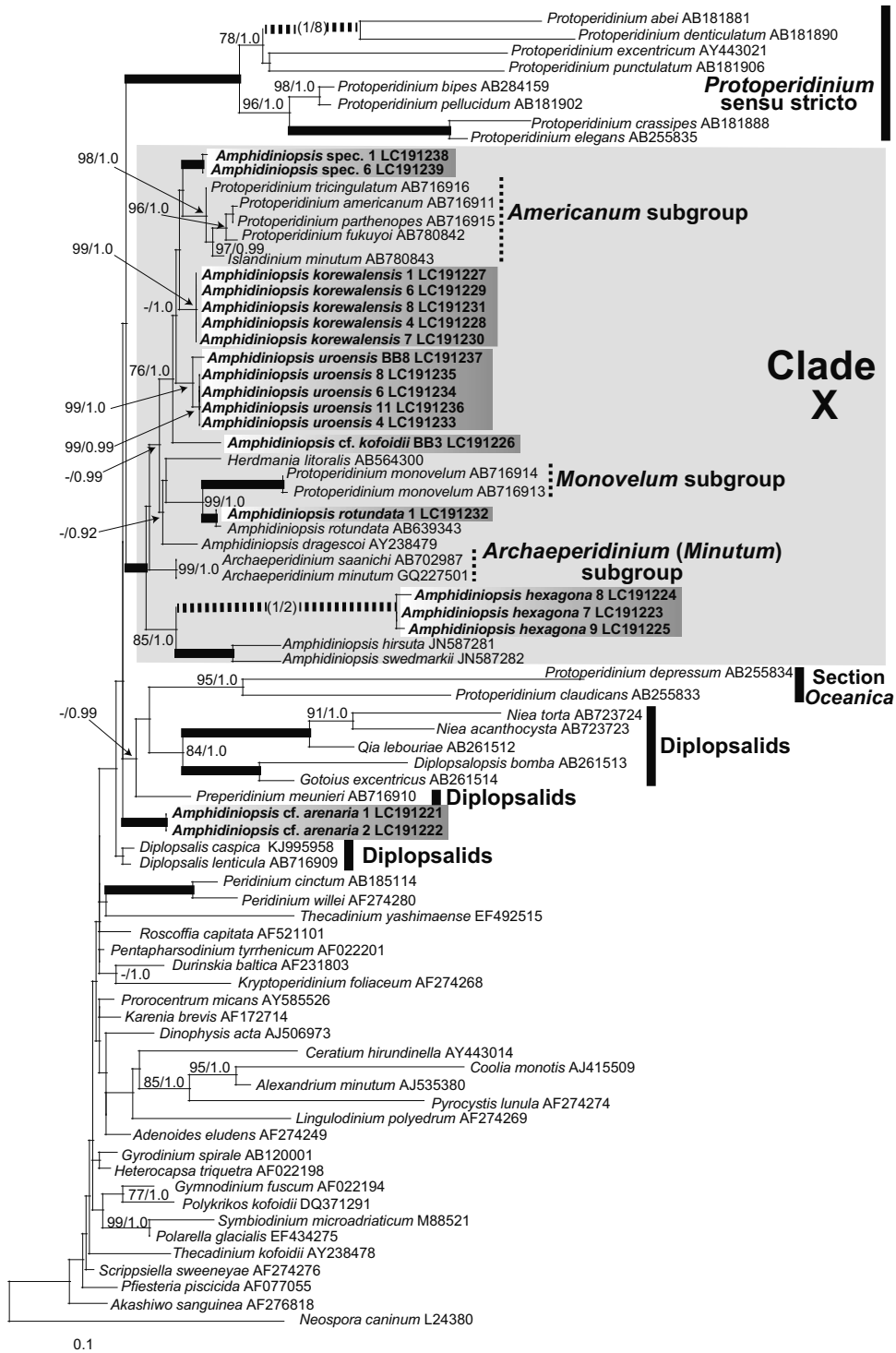


Figure 5. Maximum-likelihood (ML) tree inferred from 18S rDNA sequences. ML bootstrap values over 70% and Bayesian posterior probabilities (PP) over 0.90 are shown at the nodes (ML/PP). Thick branches indicate maximal support (100/1.00). The scale bar represents inferred evolutionary distance in changes/site. The branches leading to the fast-evolving taxa are indicated by dashed and shortened by one half and one eighth (indicated by 1/2 and 1/8), respectively. The taxa names that DNA sequences generated in this study are indicated in bold and the box of grey gradation. Clade X is indicated by the grey box. The other clades are marked with vertical lines on the right and also dashed vertical lines indicating subgroups of the *Monovela* group.

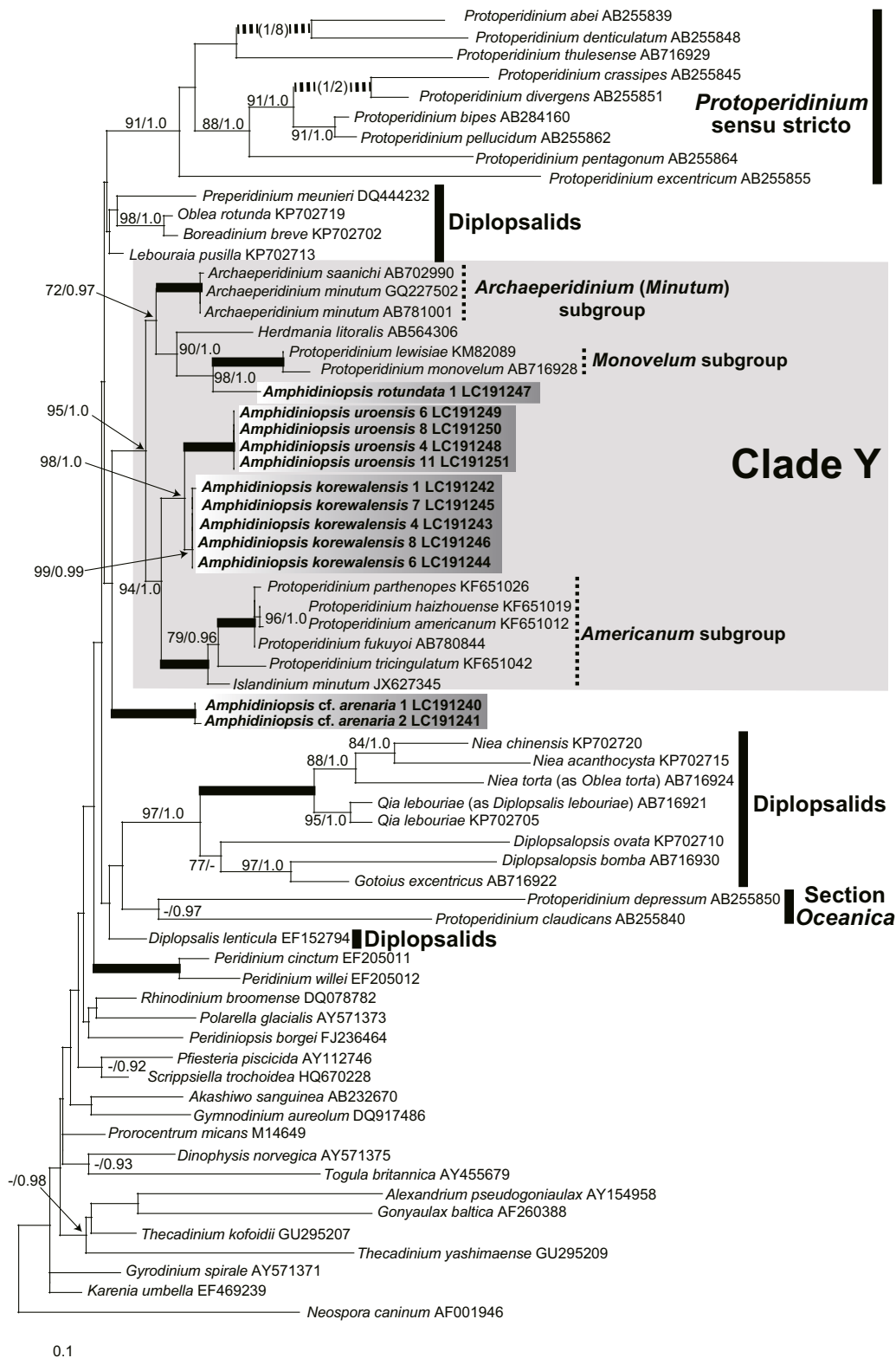


Figure 6. Maximum-likelihood (ML) tree inferred from 28S rDNA sequences. Clade Y is indicated by the grey box. Other information is the same as Figure 5.

Amphidiniopsis rotundata had strong phylogenetic affinity to *Protoperidinium monovelum* (and to *P. lewisiae* in the 28S rDNA analysis). *Protoperidinium lewisiae* was recently described by incubating the spiny round brown cysts from sediment samples in Mertens et al. (2015a). The cyst stage of *P. monovelum* has yet to be described, however, the spiny round brown cyst was reported from *P. cf. monovelum* (Matsuoka and Kawami 2013). To date, no cyst stages have been reported from *Amphidiniopsis* species. *Amphidiniopsis rotundata*, *P. monovelum* and *P. lewisiae* share the plate formula APC, 4', 3a, 7'', 5''', 2'''' (Abé 1936; Hoppenrath et al. 2012; Mertens et al. 2015a; Table 2). However, *P. monovelum* and *P. lewisiae* have four cingular plates, while *A. rotundata* has five cingular plates (Table 2). The number of the sulcal plates also differs among these species. *Amphidiniopsis rotundata* has five or six sulcal plates; *P. monovelum* has five and *P. lewisiae* has four (Table 2). *Protoperidinium monovelum*, *P. lewisiae* and *A. rotundata* also share a similar ventral area. They have a broad Sd and the sulcal fin emerges from the posterior left side of Sd (Abé 1936; Hoppenrath et al. 2012; Mertens et al. 2015a).

Analysis of the 28S rDNA dataset in this study resulted in the sand-dwelling *H. litoralis* being positioned at the base of this *A. rotundata*/*P. monovelum*/*P. lewisiae* clade (Fig. 6). Results from the 18S rDNA dataset were congruent with this finding, albeit with low statistical support (Fig. 5). From a morphological perspective, *H. litoralis* differs from *A. rotundata*, *P. monovelum*, *P. lewisiae* in that it is dorsoventrally flattened with a distinct apical hook. However, *H. litoralis* also shares the plate formula APC, 4', 3a, 7'', 5''', 2'''' (Table 2, Hoppenrath et al. 2012; Yamaguchi et al. 2011). The numbers of the cingular and sulcal plates of *H. litoralis* have yet to be clearly determined (Hoppenrath et al. 2012; Yamaguchi et al. 2011).

Amphidiniopsis hexagona, *A. hirsuta* and *A. swedmarkii* formed a moderately supported clade (Fig. 5). We could not obtain the data of these three species for the 28S rDNA analysis. According to the morphological groups proposed by Hoppenrath et al. (2012, 2014) (i.e. Group 1, 2 and 3), Group 2 contained dorsoventrally flattened *Amphidiniopsis* species with a complete cingulum and the sulcus positioned in the middle of the cell, with no apical hook, and one or two anterior intercalary plates. Among the *Amphidiniopsis* species analyzed in the present study, *A. hexagona*, *A. hirsuta* and *A. swedmarkii* belong to Group 2 and their monophyly was relatively well-supported in the 18S rDNA phylogenetic analyses (Fig. 5).

The morphology of *A. uroensis* is similar to that of *A. pectinaria*. We identified our specimen from Japan as *A. uroensis* because of the absence of the pectinated ornamentation on the two antapical plates, which is typical for *A. pectinaria* (Toriumi et al. 2002), and the presence of the “3” shape in the left edge of the Sd (Fig. 3C) which is also observed in *A. uroensis* from the northwestern Sea of Japan (See fig. 2Cd in Selina and Hoppenrath 2013). SEM observations of the Canadian isolate of *A. uroensis* (Fig. 4A) clearly showed the absence of the pectinated ornamentation on the two antapical plates.

Amphidiniopsis uroensis and *A. korewalensis* are classified in Group 3, which includes the species that have dorsoventrally flattened cells with a characteristic sulcus, an apical hook pointing to the left, and three anterior intercalary plates (Hoppenrath et al. 2012, 2014). In the 28S rDNA analysis, *A. uroensis* and *A. korewalensis* formed a clade, and this clade had a sister relationship with the members of the *Americanum* subgroup comprising *Protoperidinium americanum*, *P. fukuyoi*, *P. haizhouense*, *P. parthenopes*, *P. tricingulatum* and *Islandinium minutum* (Fig. 6).

On the other hand, the 18S rDNA phylogeny, which contained additional taxa such as *Amphidiniopsis* spec. and *A. cf. kofoidii*, did not contain a monophyletic grouping of *A. uroensis* and *A. korewalensis* (Fig. 5). These four *Amphidiniopsis* species and the *Americanum* subgroup comprised a moderately supported clade (Fig. 5). We could not find morphological characters that distinguished those species from others. The phylogenetic relationship among *A. uroensis* and *A. korewalensis* (Group 3) and the *Americanum* subgroup needs to be verified with more taxa for both 18S and 28S rDNA analyses.

Hoppenrath et al. (2012, 2014) mentioned that *A. dragescoi* might belong to Group 3, but it did not have an apical hook. The present phylogenetic result showed that *A. dragescoi* was included in Clade X, but this phylogenetic result did not show a clear phylogenetic affinity to this particular clade. The genus *Archaeperidinium* was also not clearly grouped in Clade X or Y (Figs 5, 6). *Amphidiniopsis* spec. has been reported from Russia and Germany (Selina and Hoppenrath 2013), but a detailed species description has yet to be completed.

In the present study, *Amphidiniopsis cf. arenaria* and *A. cf. kofoidii* had laterally flattened cells, and were thus categorized as belonging to Group 1 (Hoppenrath et al. 2012, 2014). For the purpose of obtaining DNA data, we could not dissect the cells of *A. cf. arenaria* nor fix and observe them under a

Table 2. Possible plate interpretations (plate formulas) of selected dinoflagellates.

	APC	'	a	"	'x'	c	s	'''	p	''''	References
<i>Amphidiniopsis</i>	APC	3-4	1-3	6-8		3-8	3-5	5	2	2	Hoppenrath et al. (2009, 2014)
<i>Amphidiniopsis rotundata</i>	APC	4	3	7		5	5(6)	5	2	2	Hoppenrath et al. (2012)
<i>Protoperidinium monovelum</i>	APC	4	3	7		4	5	5	2	2	Abé (1936); Mertens et al. (2013)
<i>Protoperidinium lewisiae</i>	APC	4	3	7		4	4	5	2	2	Mertens et al. (2015a)
<i>Herdmania litoralis</i>	APC	4	2	6	'x'	7	3	6	1	1	Hoppenrath (2000a)
<i>Herdmania litoralis</i>	APC	4	3	7		?	5-6?	5	2	2	Yamaguchi et al. (2011)
<i>Herdmania litoralis</i>	APC	4	3	7		5?	4-5?	5	2	2	Hoppenrath et al. (2012)
<i>Amphidiniopsis hexagona</i>	APC	4	2	7		3	4+2 acc.	5	2	2	Yoshimatsu et al. (2000)
<i>Amphidiniopsis hexagona</i>	APC	4	2	7		3	4	5	2	2	Hoppenrath et al. (2009)
<i>Amphidiniopsis hirusta</i>	APC	4	2	7		8	4?	5	2	2	Hoppenrath et al. (2014)
<i>Amphidiniopsis swedmarkii</i>	APC	4	2	7		3	4+2 acc.	5	2	2	Yoshimatsu et al. (2000)
<i>Amphidiniopsis swedmarkii</i>	APC	4	1	7		6?	5	5	2	2	Hoppenrath et al. (2014)
<i>Amphidiniopsis korewalensis</i>	APC	4	3	6	'x'	4?	4	6	2	2	Murray and Patterson (2002)
<i>Amphidiniopsis korewalensis</i>	APC	4	3	6		4?	4	5	2	2	Hoppenrath et al. (2012)
<i>Amphidiniopsis uroensis</i>	APC	3	3	6		3	4+1 acc.	5	2	2	Toriumi et al. (2002)
<i>Amphidiniopsis uroensis</i>	APC	3	3	6		3	5	5	2	2	Hoppenrath et al. (2012); Selina and Hoppenrath (2013)
<i>Amphidiniopsis pectinaria</i>	APC	4	3	7		3	4+1 acc.	5	2	2	Toriumi et al. (2002)
<i>Amphidiniopsis pectinaria</i>	APC	4	3	6		3	6	5	2	2	Hoppenrath et al. (2012); Selina and Hoppenrath (2013)
<i>Protoperidinium americanum</i>	APC	4	4	7		4	7	5	2	2	Lewis and Dodge (1987); Mertens et al. (2013)
<i>Protoperidinium fukuyoi</i>	APC	4	3	7		4	6	5	2	2	Mertens et al. (2013)
<i>Protoperidinium haizhouense</i>	APC	4	3	7		3	6	5	2	2	Liu et al. (2013)
<i>Protoperidinium parthenopes</i>	APC	4	3	7		4	6	5	2	2	Zingone and Montresor (1988)
<i>Protoperidinium tricingulatum</i>	APC	4	2	7		3	6?	5	2	2	Mertens et al. (2013)
<i>Islandinium minutum</i>	APC	4	2	6-7		3	5	5	2	2	Potvin et al. (2013)
<i>Amphidiniopsis dragescoi</i>	APC	4	3	7	'x'	6(7)	?	5	2	2	Hoppenrath et al. (2004)
<i>Amphidiniopsis dragescoi</i>	APC	4	3	7		6(7)	4?	4	2	2	Hoppenrath et al. (2012)
<i>Amphidiniopsis dragescoi</i>	APC	4	3	7		5/6?	4?	4	2	2	Hoppenrath et al. (2014)
<i>Amphidiniopsis arenaria</i>	APC	4	3	7		6?	4?	5	2	2	Hoppenrath (2000b)
<i>Amphidiniopsis arenaria</i>	APC	4	3	8		6	3	5	2	2	Selina and Hoppenrath (2008)
<i>Amphidiniopsis arenaria</i>	APC	4	3	7		6	4	5	2	2	Selina and Hoppenrath (2013)
<i>Amphidiniopsis kofoidii</i>	APC	4	3	7		3	3?	5	2	2	Dodge and Lewis (1986)

Abbreviations: APC, apical pore complex; ', apical plate; a, anterior intercalary plate; ", precingular plate; 'x', 'x' plate; c, cingular plate; s, sulcal plate; ''', postcingular plate; p, antapical intercalary plate; ''''', antapical plate, acc; accessory plate.

scanning electron microscope. Therefore, we could neither determine the detailed thecal plate pattern nor ornamentation for our specimen. However, the shape of the whole cell and the character of the cingulum and the sulcus were very similar to *A. arenaria* as described in Hoppenrath (2000b), Selina and Hoppenrath (2008) and Selina and Hoppenrath (2013).

Based on this contemporary expectation for the species (i.e., laterally flattened, likely with smooth thecal plates, with pores and without an apical hook), we identified our specimen as *A. cf. arenaria*. *Amphidiniopsis cf. kofoidii* (Fig. 4E, F). As the original description was incomplete regarding the thecal tabulation and ambiguous in respect to the thecal ornamentation (Włoszyńska 1928), any identification would be tentative, pending a re-investigation at the type locality (Hoppenrath et al. 2014).

In this study, *A. cf. arenaria* and *A. cf. kofoidii* did not have a close relationship. Furthermore, *A. cf. arenaria* did not fall into Clade X nor Y (Figs 5, 6), and *A. cf. kofoidii* had a moderately supported affinity with *Amphidiniopsis spec.*, *A. korewalensis*, *A. uroensis* and the *Americanum* subgroup (Fig. 5). Since *A. kofoidii* is the type species of the genus *Amphidiniopsis*, the phylogenetic position of Group 1 (*A. kofoidii*) is of taxonomic interest for the group. The detailed thecal pattern and the ornamentation of *A. cf. arenaria* with the phylogenetic data need to be further studied.

Our study suggests that the sand-dwelling genus *Amphidiniopsis* is paraphyletic and its taxonomy needs to be reconsidered in this light. Since our present phylogenetic study suggested a close and complicated relationship between these taxonomical groups, the taxonomy of the sand-dwelling genus *Amphidiniopsis* and the planktonic and cyst-producing family Protoperidiniaceae needs to be reconsidered with respect to each other.

Methods

Sampling: Sand samples containing *Amphidiniopsis* spp. were collected during low tide. The detailed sampling information for each species is shown in Table 1. The sand samples containing *Amphidiniopsis cf. arenaria* and *A. rotundata* were collected at Kannoura (33° 32' 20" N, 134° 17' 26" E), Kochi Prefecture, Japan on 18 April 2014; *Amphidiniopsis hexagona* (34° 13' 36" N, 133° 36' 36" E) was collected at Ohama, Kagawa Prefecture, Japan on 21 August 2014; *Amphidiniopsis korewalensis* was collected in a moat, Tamamo-jyo (Tamamo Castle) (34° 21' 0" N, 134° 3' 1" E), Kagawa Prefecture, Japan on 5 October 2014. *Amphidiniopsis uroensis* was collected at Suma-no-ura (34° 38' 29" N, 135° 6' 53" E) and Maiko (34° 37' 38" N, 135° 2' 24" E), Kobe, Hyogo Prefecture, Japan on 30 April 2014. *Amphidiniopsis cf. kofoidii* and *Amphidiniopsis uroen-*

sis from Canada were collected and extracted as described in Hoppenrath et al. (2012) at Boundary Bay, BC, Canada (49° 0.0' N, 123° 8.0' W) on 16 April 2007, and *Amphidiniopsis spec.* at Sandcut Beach (48° 4.2' N, 124° 0.1' W), Vancouver Island, Canada (48° 42.04' N, 124° 05.46' W) on 16 June 2007.

Isolation and light microscopical observation of *Amphidiniopsis* cells: In the laboratory, the "Uhlrig method" was used to separate flagellates from the sand (Hoppenrath et al. 2014; Uhlrig 1964). Single live cells of *Amphidiniopsis* spp. were isolated and washed three times in serial drops of 0.22 µm filtered and sterilized seawater by micropipetting, using a ZEISS Primovert microscope (Zeiss, Jena, Germany), transferred to a glass slide with a vinyl tape frame (Horiguchi et al. 2000) and sealed with a cover glass. Each cell then was observed using a BX-50 compound microscope with Nomarski optics (Olympus, Tokyo, Japan) equipped with a VB-7000 digital camera (Keyence, Tokyo, Japan), identified to species and photographed for future record. Some cells were stained with Calcofluor White Stain (Sigma-Aldrich, St. Louis, MO, USA) and observed with an Olympus BX epifluorescent microscope (Olympus). After a photographic record had been made, each cell was transferred to a 200 µL PCR tube containing 10 µL of Quick Extract FFPE DNA Extraction Solution (Epicentre, Madison, WI, USA) and incubated for 1 h at 56 °C, then for 2 min at 98 °C. The resulting extract was used as a DNA template for PCR amplification. In Canada several cells of a population of a species were washed three times in sterile f/2-medium and genomic DNA was extracted using the MasterPure Complete DNA and RNA purification kit (Epicentre). For *A. cf. kofoidii* and *A. spec* six cells and for *A. uroensis* 2 cells were used.

Single-cell polymerase chain reaction (SC-PCR) and sequencing: The initial PCR was performed using a total volume of 25 µL with EconoTaq 2X Master Mix (error rate 1 per 20,000-40,000) (Lucigen, Middleton, WI, USA) or KOD FX (error rate 1 per 50,000) (ToYoBo, Osaka, Japan) following the manufacture's protocols. Nearly the entire 18S rRNA gene and the part of the 28S rRNA gene were amplified using the sets of universal eukaryote primers: (SR1: 5'-TACCTGGTTGATCCTGCCAG-3', 25F1: 5'-CCGCTGAATTTAAGCATAT-3' and LSU R2: 5'-ATTCGGCAGGTGAG TTGTTAC-3') or (SR1: 5'-TACCTGGTTGATCCTGCCAG-3' and 28-1483R: 5'-GCTACTACCACCAAGATCTGC-3') (Daugbjerg et al. 2000; Kogame et al. 1999; Takano and Horiguchi 2004). The PCR protocol for EconoTaq 2X Master Mix had an initial denaturation stage at 94 °C for 2 min; 30 cycles of denaturation at 94 °C for 30 s, annealing at 48 °C for 30 s, and extension at 72 °C for 3 min 30 s; and final extension at 72 °C for 7 min. The PCR protocol for KOD FX had an initial denaturation stage at 94 °C for 2 min; 35 cycles of denaturation at 98 °C for 10 s, annealing at 50 °C for 30 s, and extension at 68 °C for 2-4 min; and final extension at 72 °C for 30 sec. The first PCR product was used as a DNA template for the second semi-nested or nested PCR. The second PCR was performed using EconoTaq 2X Master Mix where the following combinations of primer pairs were used separately: SR1 and SR12, SR1 and SR9p, SR4 and SR12, 25F1 and LSU R2 (Nunn et al. 1996; Takano and Horiguchi 2004; Yamaguchi et al. 2006) with the same PCR protocol with the initial PCR except for the shorter extension time (1.5-2 min). Using the second PCR products as the template DNA, the third PCR was conducted using EconoTaq 2X Master Mix by the following combinations of primer pairs: SR1 and SR5TAK, SR4 and SR9p, SR8p and SR12, 25F1 and 25R1, D3A and LSU R2 (Mertens et al. 2013) Thermal cycling was conducted using an initial denaturation stage at 94 °C for 2 min, followed by 25 cycles of 94 °C for 30 s, annealing at 50 °C

for 30 s, and extension at 72 °C for 30 s, and final extension at 72 °C for 7 min. Amplified DNA fragments corresponding to the expected size were separated by agarose gel electrophoresis and cleaned using the UltraClean™ 15 DNA Purification Kit (Mo Bio Laboratories, Carlsbad, CA, USA) or QIAquick PCR Purification Kit (QIAGEN, Hilden, Germany). The cleaned PCR products were sequenced directly by Fasmac sequencing service (Fasmac, Kanagawa, Japan). In Canada 18S rDNA sequences were PCR amplified using puReTaq Ready-to-go PCR beads (GE Healthcare, Quebec, Canada), with an error rate of 1 per 20,000–40,000 bases, and universal eukaryotic primers (*A. spec.*: PF1-R4, *A. cf. kofoidii* and *A. uroensis*: PF1-MetnonR). The PCR product of the expected size was gel isolated and cloned into pCR2.1 vector using a TOPO TA cloning kit (Invitrogen, Carlsbad, CA, USA). One clone was completely sequenced with ABI big-dye reaction mix using both vector primers and two internal primers oriented in both directions. New sequences have been deposited in DDBJ/EMBL/GenBank under the accession numbers listed in Table 1.

Sequence alignments and phylogenetic analyses: The 18S and 28S rDNA sequences were aligned using “MUSCLE” (Edgar 2004; <http://www.ebi.ac.uk/Tools/msa/muscle/>), respectively, with the default settings and then manually refined in Mesquite version 3.03 (Maddison and Maddison 2015). The final alignment of the 18S rDNA dataset consisted of 78 taxa and 1,191 sites. The final alignment of 28S rDNA sequences including the domains D1–D3, excluding hypervariable regions, consisted of 67 taxa and 645 sites. The apicomplexan *Neospora caninum* was used as the outgroup for both datasets. The alignments are available from the corresponding author upon request. Phylogenetic trees were constructed using maximum likelihood (ML) and Bayesian analysis. For ML, the alignments were analyzed by GARLI version 0.951 (Zwickl 2006). The GTR+I+G model of nucleotide substitution was chosen by the Akaike Information Criterion as implemented in jModelTest 2.1.4. for both datasets (Darriba et al. 2012; Guindon and Gascuel 2003). The parameters were as follows: for 18S rDNA dataset, assumed nucleotide frequencies were A=0.2451, C=0.2081, G=0.2488, T=0.2980; substitution rate matrix with A–C substitutions = 1.1072, A–G = 4.7586, A–T = 1.2806, C–G = 0.6907, C–T = 8.3513, G–T = 1.0000; proportion of sites assumed to be invariable = 0.2850 and rates for variable sites assumed to follow a gamma distribution with shape parameter = 0.5590. For 28S rDNA dataset, assumed nucleotide frequencies were A=0.2622, C=0.1839, G=0.2788, T=0.2751; substitution rate matrix with A–C substitutions = 1.3320, A–G = 4.0492, A–T = 1.2608, C–G = 0.6596, C–T = 8.6391, G–T = 1.0000; proportion of sites assumed to be invariable = 0.1690 and rates for variable sites assumed to follow a gamma distribution with shape parameter = 1.0490. Bootstrap analyses were carried out for ML with 500 replicates to evaluate statistical reliability. MrBayes version 3.2.5 was used to perform Bayesian analyses (Ronquist and Huelsenbeck 2003) with the GTR+I+gamma evolutionary model for both 18S and 28S rDNA datasets. The program was set to operate four Monte-Carlo-Markov chains (MCMC) starting from a random tree. A total of 1,500,000 generations (18S rDNA) and 1,000,000 generations (28S rDNA) were calculated with trees sampled every 100 generations. The first 3,750 (18S rDNA) and 2,500 (28S rDNA) trees in each run were discarded as burn-in. Posterior probabilities (PP) correspond to the frequency at which a given node was found in the post-burn-in trees.

Acknowledgements

This work was supported by Supporting Positive Activities for Female Researchers on ‘Revolution! Female Researcher Training “Kobe Style”’ at Kobe University financed by Japan Science and Technology Agency, Japan.

References

- Abé TH (1936) Report of the biological survey of Mutsu Bay. 29. Notes on the protozoan fauna of Mutsu Bay. II. Genus *Peridinium*; subgenus *Archaeperidinium*. Science Reports of Tohoku University 4th Series, Biology 10:639–686
- Abé TH (1981) Studies on the Family Peridiniidae. An Unfinished Monograph of Armoured Dinoflagellata vol. VI, Publications of the Seto Marine Biological Laboratory, Special Publication Series, pp 1–413
- Darriba D, Taboada GL, Doallo R, Posada D (2012) jModelTest 2: more models, new heuristics and parallel computing. Nat Methods 9:772
- Daugbjerg N, Hansen G, Larsen J, Moestrup Ø (2000) Phylogeny of some of the major genera of dinoflagellates based on ultrastructure and partial LSU rDNA sequence data, including the erection of three new genera of unarmoured dinoflagellates. Phycologia 39:302–317
- Dodge JD, Lewis J (1986) A further SEM study of armoured sand-dwelling marine dinoflagellates. Protistologica 22:221–230
- Edgar RC (2004) MUSCLE: multiple sequence alignment with high accuracy and high throughput. Nucleic Acids Res 32:1792–1797
- Gómez F, López-García P, Moreira D (2011) Molecular phylogeny of the sand-dwelling dinoflagellates *Amphidiniopsis hirsuta* and *A. swedmarkii* (Peridinales, Dinophyceae). Acta Protozool 50:255–262
- Guindon S, Gascuel O (2003) A simple, fast and accurate method to estimate large phylogenies by maximum-likelihood. Syst Biol 52:696–704
- Hoppenrath M (2000a) An emended description of *Herdmania litoralis* Dodge (Dinophyceae) including the plate formula. Nova Hedwigia 71:481–490
- Hoppenrath M (2000b) Morphology and taxonomy of six marine sand-dwelling *Amphidiniopsis* species (Dinophyceae, Peridinales), four of them new, from the German Bight, North Sea. Phycologia 39:482–497
- Hoppenrath M, Koeman RPT, Leander BS (2009) Morphology and taxonomy of a new marine sand-dwelling *Amphidiniopsis* species (Dinophyceae, Peridinales), *A. aculeata* sp. nov., from Cap Ferret, France. Mar Biodivers 39:1–7
- Hoppenrath M, Murray SA, Chomérat N, Horiguchi T (2014) Marine Benthic Dinoflagellates –Unveiling their Worldwide Biodiversity. Kleine Senckenberg-Reihe, Band 54, Schweizerbart, Stuttgart, Germany, 276 p

- Hoppenrath M, Selina M, Yamaguchi A, Leander BS** (2012) Morphology and molecular phylogeny of *Amphidiniopsis rotundata* sp. nov. (Peridinales Dinophyceae), a benthic marine dinoflagellate. *Phycologia* **51**:157–167
- Hoppenrath M, Saldarriaga JF, Schweikert M, Elbrächter M, Taylor FJR** (2004) Description of *Thecadinium mucosum* sp. nov. (Dinophyceae), a new sand-dwelling marine dinoflagellate, and an emended description of *Thecadinium inclinatum* Balech. *J Phycol* **40**:946–961
- Horiguchi T, Yoshizawa-Ebata J, Nakayama T** (2000) *Halostylodinium arenarium*, gen. et sp. nov. (Dinophyceae), a coccoid sand-dwelling dinoflagellate from subtropical Japan. *J Phycol* **36**:960–971
- Kawami H, van Wezel R, Koeman RPT, Matsuoka K** (2009) *Protoperidinium tricingulatum* sp. nov. (Dinophyceae), a new motile form of a round, brown, and spiny dinoflagellate cyst. *Phycol Res* **57**:259–267
- Kogame K, Horiguchi T, Masuda M** (1999) Phylogeny of the order Scytosiphonales (Phaeophyceae) based on DNA sequences of *rbcL*, partial *rbcS*, and partial LSU nrDNA. *Phycologia* **38**:496–502
- Lewis J, Dodge JD** (1987) The cyst-theca relationship of *Protoperidinium americanum* (Gran and Braarud) Balech. *J Micropalaeontol* **6**:113–121
- Liu T, Gu H, Mertens KN, Lan D** (2013) A new dinoflagellate species *Protoperidinium haizhouense* sp. nov. (Peridinales Dinophyceae), its cyst-theca relationship and phylogenetic position within the *Monovela* group. *Phycol Res* **62**:109–124
- Liu Y, Mertens KN, Ribeiro S, Ellegaard M, Matsuoka K, Gu H** (2015) Cyst-theca relationships and phylogenetic positions of Peridinales (Dinophyceae) with two anterior intercalary plates, with description of *Archaeoperidinium bailongense* sp. nov. and *Protoperidinium fuzhouense* sp. nov. *Phycol Res* **63**:134–151
- Maddison WP, Maddison DR** (2015) Mesquite: a Modular System for Evolutionary Analysis. Version 3.03. <http://mesquiteproject.org>
- Matsuoka K, Kawami H** (2013) Phylogenetic Subdivision of the Genus *Protoperidinium*, (Peridinales, Dinophyceae) with Emphasis on the *Monovela* Group. In Lewis JM, Marret F, Bradley L (eds) *Biological and Geological Perspectives of Dinoflagellates*. The Micropalaeontological Society, Special Publications. Geological Society, London, pp 267–276
- Mertens KN, Tanano Y, Gu H, Yamaguchi A, Pospelova V, Ellegaard M, Matsuoka K** (2015a) Cyst-theca relationship of a new dinoflagellate with a spiny round brown cyst, *Protoperidinium lewisiae* sp. nov., and its comparison to the cyst of *Oblea acanthocysta*. *Phycol Res* **63**:110–124
- Mertens KN, Takano Y, Yamaguchi A, Gu H, Bogus K, Kremp A, Bagheri S, Matishov G, Matsuoka K** (2015b) The molecular characterization of the enigmatic dinoflagellate *Kolkwitzella acuta* reveals an affinity to the *Excentrica* section of the genus *Protoperidinium*. *Syst Biodivers* **13**:509–524
- Mertens KN, Yamaguchi A, Kawami H, Ribeiro S, Leander BS, Price AM, Pospelova V, Ellegaard M, Matsuoka K** (2012) *Archaeoperidinium saanichi* sp. nov.: a new species based on morphological variation of cyst and theca within the *Archaeoperidinium minutum* Jörgensen 1912 species complex. *Mar Micropaleontol* **96**:48–62
- Mertens KN, Yamaguchi A, Takano Y, Pospelova V, Head MJ, Radi T, Pienkowski AJ, Vernal A, Kawami H, Matsuoka K** (2013) A new heterotrophic dinoflagellate from the Northeastern Pacific, *Protoperidinium fukuyoi*: cyst-theca relationship, phylogeny, distribution and ecology. *J Eukaryot Microbiol* **60**:545–563
- Murray S, Patterson DJ** (2002) *Amphidiniopsis korewalensis* sp. nov., a new heterotrophic benthic dinoflagellate. *Phycologia* **41**:382–388
- Nunn GB, Theisen BF, Christensen B, Arctander P** (1996) Simplicity-correlated size growth of the nuclear 28S ribosomal RNA D3 expansion segment in the crustacean order Isopoda. *J Mol Evol* **42**:211–223
- Potvin É, Rochon A, Lovejoy C** (2013) Cyst-theca relationship of the arctic dinoflagellate cyst *Islandinium minutum* (Dinophyceae) and phylogenetic position based on SSU rDNA and LSU rDNA. *J Phycol* **49**:848–866
- Ribeiro S, Lundholm N, Amorim A, Ellegaard M** (2010) *Protoperidinium minutum* (Dinophyceae) from Portugal: cyst-theca relationship and phylogenetic position on the basis of single-cell SSU and LSU rDNA sequencing. *Phycologia* **49**:48–63
- Ronquist F, Huelsenbeck JP** (2003) MRBAYES 3: Bayesian phylogenetic inference under mixed models. *Bioinformatics* **19**:1572–1574
- Selina MS, Hoppenrath M** (2008) An emended description of *Amphidiniopsis arenaria* Hoppenrath 2000, based on material from the Sea of Japan. *Europ J Protistol* **44**:71–79
- Selina MS, Hoppenrath M** (2013) Morphology and taxonomy of seven marine sand-dwelling *Amphidiniopsis* species (Peridinales, Dinophyceae), including two new species *A. konovalovae* sp. nov. and *A. striata* sp. nov., from the Sea of Japan, Russia. *Mar Biodivers* **43**:87–104
- Takano Y, Horiguchi T** (2004) Surface ultrastructure and molecular phylogenetics of four unarmoured heterotrophic dinoflagellates, including the type species of the genus *Gyrodinium* (Dinophyceae). *Phycol Res* **52**:107–116
- Toriumi S, Yoshimatsu S, Dodge JD** (2002) *Amphidiniopsis uroensis* sp. nov. and *Amphidiniopsis pectinaria* sp. nov. (Dinophyceae): two new benthic dinoflagellates from Japan. *Phycol Res* **50**:115–124
- Uhlig G** (1964) Eine einfache Methode zur Extraktion der vagilen, mesopsammalen Mikrofauna. *Helgol wiss Meeresunters* **11**:178–185
- Yamaguchi A, Kawamura H, Horiguchi T** (2006) A further phylogenetic study of the heterotrophic dinoflagellate genus, *Protoperidinium* (Dinophyceae) based on small and large subunit ribosomal RNA gene sequences. *Phycol Res* **54**:317–329
- Yamaguchi A, Hoppenrath M, Pospelova V, Horiguchi T, Leander BS** (2011) Molecular phylogeny of the marine sand-dwelling dinoflagellate *Herdmania litoralis* and an emended description of the closely related planktonic genus *Archaeoperidinium* Jörgensen. *Eur J Phycol* **46**:98–112
- Wołoszyńska J** (1928) Dinoflagellates der polnischen Ostsee sowie der an Piasnica gelegenen Sumpfe. *Arch Hydrobiol Rybact* **3**:153–278
- Yoshimatsu S, Toriumi S, Dodge JD** (2000) Light and scanning microscopy of two benthic species of *Amphidiniopsis*

(Dinophyceae), *Amphidiniopsis hexagona* sp. nov. and *Amphidiniopsis swedmarkii* from Japan. *Phycol Res* **48**:107–113

Zingone A, Montresor M (1988) *Protoperidinium parthenopes* sp. nov. (Dinophyceae), an intriguing dinoflagellate from the Gulf of Naples. *Cryptogamie Algologie* **9**:117–125

Zwickl DJ (2006) Genetic algorithm approaches for the phylogenetic analysis of large biological sequence datasets under the maximum likelihood criterion Ph. D. dissertation. The University of Texas, Austin, Austin, TX

Available online at www.sciencedirect.com

ScienceDirect